

Microstructure and Mechanical Properties of C_f/SiC Composites Reinforced with Boron Nitride Nanowires

G. Zhu^{1, 2, 3}, S. Dong^{*1, 2}, J. Hu^{1, 2}, Y. Kan^{1, 2},
L. Gao^{1, 2}, X. Zhang^{1, 2}, Z. Wang^{1, 2}, Y. Ding^{1, 2}

¹State Key Laboratory of High Performance Ceramics and Superfine Microstructure, Shanghai Institute of Ceramics, Chinese Academy of Sciences, Shanghai 200050, China

²Structural Ceramics and Composites Engineering Research Center, Shanghai Institute of Ceramics, Chinese Academy of Sciences, Shanghai 200050, China

³University of Chinese Academy of Sciences, Beijing 100049, China

received August 31, 2016; received in revised form October 20, 2016; accepted November 11, 2016

Abstract

Boron nitride nanowires (BNNWs) were first grown *in situ* into fiber preforms, and then C_f/SiC composites reinforced with the BNNWs were fabricated by means of chemical vapor infiltration (CVI) matrix densification. It was found that thanks to the incorporation of the BNNWs, the matrix of the C_f/SiC composites at micron scale is toughened notably, as evidenced by the results of indentation tests. Synergetic strengthening and toughening mechanisms including debonding, fracture, pullouts as well as crack branching and deflection attributed to BNNW-based micro-rods are observed. However, no significant increases in flexural strength and fracture toughness are obtained for the composites, possibly owing to the lower density of composites and strong interface bonding between the BNNWs and the matrix.

Keywords: Ceramic matrix composites, boron nitride nanowires, bending test, microindentation, toughness

I. Introduction

Because of their excellent toughness, good thermal stability and remarkable high-temperature strength, ceramic matrix composites (CMCs) are well known as highly promising candidates for high-temperature, high-stress applications in aerospace, hot engines, etc.¹⁻³. The high toughness of their matrix is generally achieved by means of appropriately controlled fiber/matrix bonding⁴. Many efforts have therefore been made to tailor the fiber/matrix interface to improve the strength and fracture tolerance of composites⁴⁻⁷. However, the matrix at micron scale among the fibers remains a brittle ceramic, resulting in crack initiation and propagation in such regions. One-dimensional nanomaterials, such as carbon nanotubes (CNTs) have tremendous potential for structural applications in composites thanks to their excellent mechanical properties⁸⁻¹⁰. CNTs have been universally introduced into CMCs as nanoscale reinforcements to their improve mechanical properties at micron scale due to their nanoscale diameters¹¹⁻¹³. Nonetheless, the further use of CNTs in CMCs is limited because of their poor oxidation resistance at temperatures above 400 °C¹⁴.

Hexagonal boron nitride (h-BN) is a promising material that possesses high mechanical strength, outstanding thermal properties and good oxidation resistance¹⁵⁻¹⁷. These merits endow one-dimensional BN nanostructures,

including boron nitride nanowires (BNNWs) and boron nitride nanotubes (BNNTs), with great potential for supplanting CNTs for use in CMCs. BNNTs have shown promising application in CMCs as nanoscale reinforcements because of their high tensile strength and elastic modulus¹⁹⁻²². The good mechanical properties are attributable to strong bonding among boron and nitrogen atoms in (002) crystal planes. BNNWs have similar structures to BNNTs, except that BNNWs are the filled cylindrical structures of BN¹⁸. Hence, it is considered that BNNWs with (002) planes parallel to the nanowire axis also have good mechanical properties and can be employed as nanoscale reinforcements in CMCs¹⁷. However, to the best of our knowledge, no findings on CMCs with incorporated BNNWs have been reported up to now.

In the present study, carbon-fiber-reinforced silicon carbide (SiC) matrix composites with incorporated BNNWs (C_f/SiC -BNNWs) were fabricated. The BNNWs were first grown *in situ* into fiber preforms, and then C_f/SiC -BNNWs were obtained by means of chemical vapor infiltration (CVI) matrix densification. The morphology, microstructure, chemical composition of the nanowires and possible growth mechanism were studied. The effects of the BNNWs on the microstructure and mechanical properties of the composites were investigated based on detailed comparative characterization of the composites with and without BNNWs.

* Corresponding author: composites@mail.sic.ac.cn

II. Experimental Procedure

C_f/SiC-BNNW composites were fabricated in the following steps: Firstly, BNNWs were grown *in situ* into fiber preforms using a simplified ball milling, impregnation and annealing method. This method was initially used for the synthesis of BNNTs on fiber cloths and has been reported in our previous study²³. 12 g h-BN powder (98.5 %, Aladdin) was ball-milled for about 120 h with 500 ml ethanol and zirconia balls in polyurethane (PU) milling vessels (1 l) at a speed of 350 rpm in a vertical planetary ball mill. The weight ratio of $\emptyset 10$ mm and $\emptyset 6$ mm milling balls is 1:1 and the balls to powder weight ratio is 60:1. The as-milled powder was mixed with 500 ml 0.04 M cobalt nitrate (Co(NO₃)₂) ethanol solution as a precursor slurry. Three-dimensional needled carbon fiber preform (Toray) with a fiber volume fraction of about 30 % was impregnated in the precursor slurry for 2 h under ultrasonic vibration. After it had been dried, the fiber preform was heat-treated in a tube furnace at 700 °C for 10 min under ammonia (NH₃) atmosphere. The Co(NO₃)₂ was decomposed into cobalt (Co) catalyst particles. The fiber preform was then heat-treated at 1300 °C for 2 h under N₂ atmosphere in a high-pressure furnace to promote *in situ* growth of the BNNWs. Subsequently, the fiber preform with the BNNWs was densified with the CVI method. The SiC matrix was deposited onto the fiber preform at 1000 °C using methyltrichlorosilane (MTS, CH₃SiCl₃) and hydrogen (H₂) as precursors, with a molar ratio of H₂ to MTS at 10:1. C_f/SiC-BNNWs composites were obtained after several CVI cycles. For comparison, C_f/SiC composites without BNNWs were fabricated using the same densification process.

The Archimedes method was employed to determine the bulk density and open porosity of the composites. The composites were machined into bar specimens with the dimensions 4.0 mm × 5.0 mm × 60 mm for flexural strength measurement. This measurement was conducted in a three-point bending test with a span of 50 mm at a cross-head speed of 0.5 mm/min. The fracture toughness was measured with the single-edge notched beam (SENB) method with a span of 20 mm. The bar specimens were prepared with the size of 2.5 mm × 5.0 mm × 26 mm (with a notch measuring 2.5 mm in depth). Both the flexural strength and fracture toughness measurements were performed on an Instron-5566 universal testing machine. The indentation was made with a triangular diamond pyramidal indenter using optic microscopy to evaluate the mechanical properties of the matrix at micron scale among the fibers. A Hitachi SU8220 field-emission scanning electron microscopy (FESEM) was used to observe the morphology of BNNWs, the polished cross-sections and fracture surfaces of the composites and the indentation. A JEM-2100F field emission transmission electron microscope (FETEM) was employed to investigate the microstructure

of the nanowires. The chemical compositions of the nanowires and the catalyst at the tip of nanowires were determined by means of X-ray energy dispersive spectroscopy (EDS) attached to FESEM.

III. Results and Discussion

As described above, BNNWs were grown *in situ* into fiber preforms using a simplified ball milling, impregnation and annealing method. It is estimated that the amount of BNNWs is about 3 wt% of the fiber preform based on the change in weight of the fiber preform before and after the growth of BNNWs. The SEM image (Fig. 1a) at low magnification shows the general morphology of BNNWs grown *in situ* into fiber preforms. It can be seen that as-grown BNNWs are not very thick but uniformly distributed on the surface of fibers. The length of the as-grown BNNWs is in the range of 1–50 μm. The enlarged image (Fig. 1b) reveals that the BNNWs have a diameter of 50–180 nm. At higher magnification (Fig. 1c), it is observed that there are some spherical particles located at the tips of the nanowires, as indicated by the white arrows in Fig. 1c. The typical EDS spectra (Fig. 1d) taken from these spherical particles indicates that these particles are Co catalyst particles. Given that catalyst particles are usually encapsulated inside the nanowires or nanotubes, the boron and nitrogen signals in Fig. 1d originate from the BN layers surrounding the particles. It also implies that these as-grown nanowires are BNNWs. The O element may be attributed to slight surface oxidation or surface oxygen adsorption of nanowires during sample preservation. The microstructures of the nanowires were further investigated with TEM, as shown in Fig. 1e–g. Fig. 1e clearly reveals that the one-dimensional nanostructures are not hollow but filled structures, confirming the success of the nanowire synthesis. Typical high-magnification TEM images of the nanowires are presented in Fig. 1f and g. It can be observed that the nanowires have clear lattice fringes, indicating excellent crystallinity of the nanowires. What is more, the lattice fringes are parallel to the axis of the nanowires, which is of great importance for achieving high mechanical strength¹⁷. The distance between the lattice fringes is ~0.335 nm, as labeled in Fig. 1g, which is consistent with the lattice constant of bulk h-BN along the c-axis. The spherical particles found at the tips of the nanowires are normally regarded as the sign of the vapor-liquid-solid (VLS) mechanism. However, there is no doubt that the growth of nanowires from vapor BN phase is impossible in the present study. According to the results reported by Chen *et al.*²⁴, Chadderton *et al.*²⁵ and Zhang *et al.*²⁶, it is considered that the boron source may arise from the h-BN powder and the solid-liquid-solid (SLS) mechanism is preferred to best comprehend the growth of nanowires. Such BNNWs grown *in situ* into fiber preforms are introduced into the matrix of composites as nanoscale reinforcements.

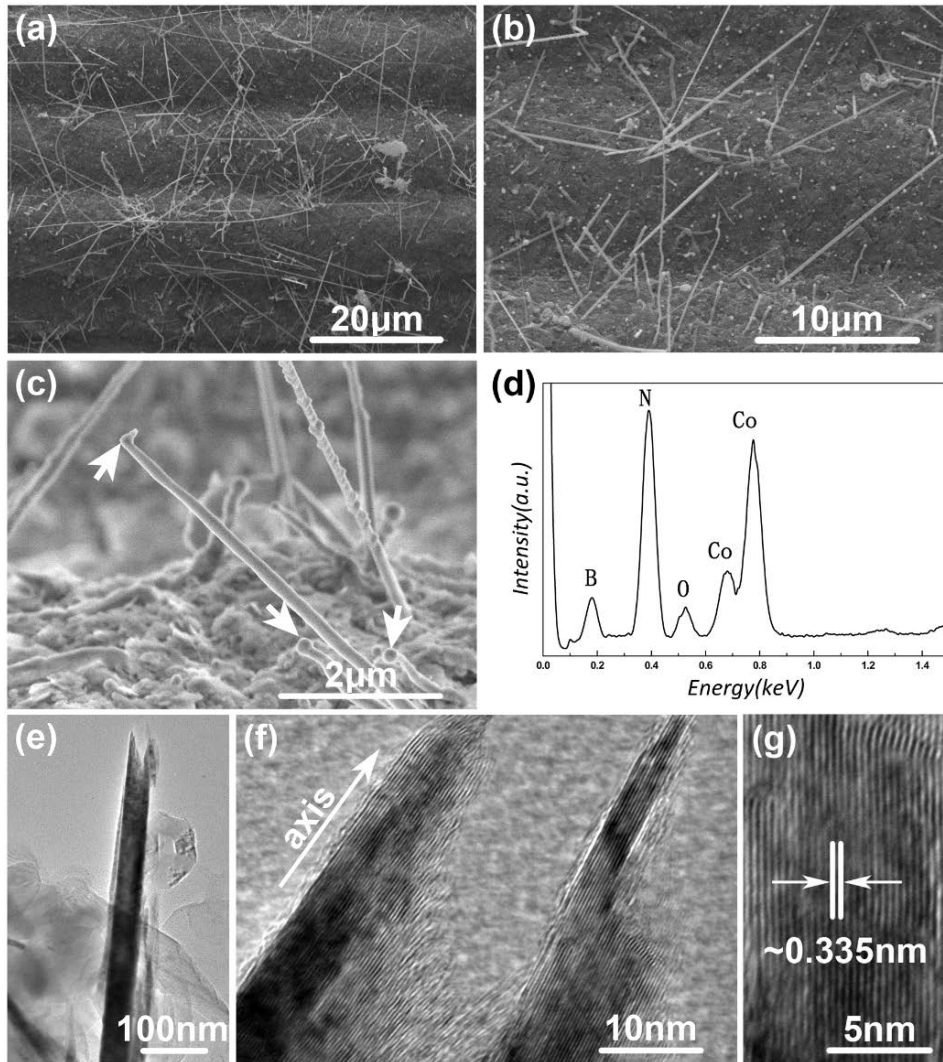


Fig. 1: (a-c) Typical SEM images of BNNWs grown *in situ* into fiber preforms. Spherical particles are observed at the tips of the nanowires, as indicated by the white arrows in the image. (d) EDS spectra of the spherical particles at the tips of the nanowires. (e-g) Typical TEM images of BNNWs. Clear lattice fringes of the nanowires are observed to be parallel to the axis of nanowires. The distance between the lattice fringes is ~0.335 nm, as labeled in the image.

Table 1: Properties of C_f/SiC composites with and without BNNTs grown *in situ* inside.

Composites	Density (g·cm ⁻³)	Open porosity (%)	σ (MPa)	σ ^{N*} (MPa/(g·cm ⁻³))	K _{IC} (MPam ^{1/2})	K _{IC} ^{N*} (MPam ^{1/2} /(g·cm ⁻³))
C _f /SiC	2.30±0.08	10.5±1.7	386.8±55.8	168.2±24.3	12.6±1.5	5.5±0.7
C _f /SiC-BNNWs	2.11±0.02	14.5±0.4	387.0±25.3	183.4±12.0	11.1±2.9	5.3±1.4

*) σ^N and K_{IC}^N are normalized flexural strength and fracture toughness by the density, respectively.

After densification with the CVI method, C_f/SiC-BN-NWs composites and C_f/SiC composites were obtained. Table 1 shows the density and open porosity of these two composites. It can be seen that with the introduction of BNNWs, the average density of the C_f/SiC composites decreases from 2.30 ± 0.08 g·cm⁻³ to 2.11 ± 0.02 g·cm⁻³ and correspondingly the open porosity increases from 10.5 ± 1.7 % to 14.5 ± 0.4 %. This might be due to the pore channels clogging effect during the CVI process. The BNNWs

divided the pore channels among the fibers into smaller ones. These smaller pore channels were sealed quickly and easily, hindering the vapor infiltration process and leaving many voids without enough matrix. It can also be affirmed from the overall morphology of the polished cross-sections of C_f/SiC-BNNWs composites as shown in Fig. 2a. Obvious voids can be found in the C_f/SiC-BNNWs composites. This situation is opposite to the result reported by Tatarko *et al.* 27. In their work, it was found that the pres-

ence of metal catalysts introduced for nanotube growth could help the densification process of zirconia ceramic by changing the sintering behavior from solid-phase to liquid-phase sintering. However, in this paper the CVI method is employed in which the vapor precursors' infiltration into the fiber preform is the key factor. Additionally, many micro-rods are observed inside these voids without enough matrix, as exhibited in the inset in Fig. 2a. Further investigation of the micro-rod is displayed in Fig. 2b, revealing that a BNNW is inside the micro-rod as the core, which is surrounded by SiC matrix deposited with the CVI method. Three layers of SiC matrix are observed outside the BNNW, which corresponds to the CVI process being conducted three times. In the back-scattered SEM images of the polished cross-sections of C_f/SiC -BNNW composites (Fig. 2c and d), black semi-circles and gray portions are readily distinguished as carbon fibers and SiC matrix, respectively. Meanwhile, many black points and lines at nanoscale that have similar color contrast to carbon fibers are also observed in the matrix among the fibers (as indicated by the white arrows in Fig. 2c). They can be easily identified as BNNWs based on the fact that the average atomic number of BN is equal to that of carbon. The above result demonstrates that BNNWs have been successfully incorporated into the matrix in C_f/SiC composites.

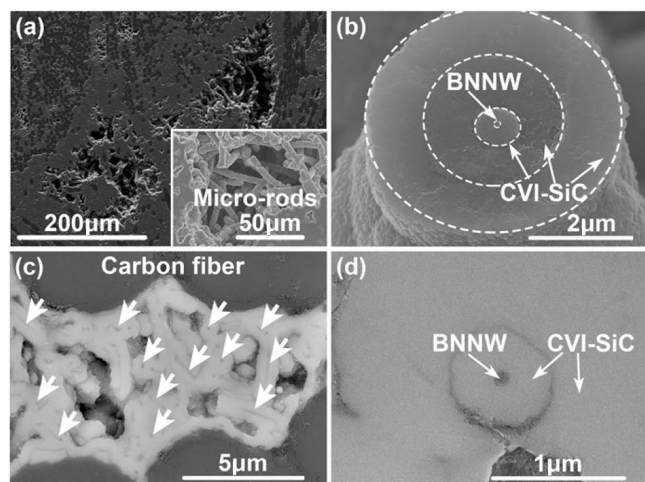


Fig. 2: (a) SEM images of the polished cross-sections of C_f/SiC -BNNWs composites. The inset displays that many micro-rods are inside the void without enough matrix. (b) SEM image of the fracture surface of the micro-rod, revealing that a BNNW is inside the rod as the core, which is surrounded by SiC matrix. (c) and (d) Back-scattered SEM images of the polished cross-section of C_f/SiC -BNNWs composites. Black points and lines, black semi-circles and other gray portions are identified as BNNWs, carbon fibers and SiC matrix, respectively, as annotated in the images.

The flexural strength and fracture toughness of the C_f/SiC -BNNW composites and C_f/SiC composites are summarized in Table 1. The C_f/SiC -BNNW composites possess an average flexural strength of 387.0 ± 25.3 MPa, which is almost equal to that of 386.8 ± 55.8 MPa for the C_f/SiC composites. In addition, the average fracture toughness of the C_f/SiC -BNNW composites is 11.1 ± 2.9 Mpa $m^{1/2}$, which is marginally lower than that of 12.6 ± 1.5 Mpa $m^{1/2}$ for the C_f/SiC composites. It seems that the incorporation of BNNWs is not conducive to

improving the mechanical properties of the C_f/SiC composites. However, if we consider the densification difference between the C_f/SiC -BNNW composites and the C_f/SiC composites, the above result can be understood. The C_f/SiC -BNNW composites are not fully densified with SiC matrix, and voids in the composites inevitably impair the effective load-carrying area, resulting in the reduction of mechanical properties. Namely, the positive effect of BNNWs may be offset by the poor densification of composites. According to the findings reported by Yang *et al.*⁸, the mechanical properties could be simply normalized by density by calculating the ratio of the mechanical properties (such as flexural strength and fracture toughness) and the density. By doing this, the disturbance arising from the different densities of samples could be ruled out and the real contribution of SiC nanowires in C_f/SiC composites could be determined. As a reference, the mechanical properties were also normalized by the density in the present study. The flexural strength of the C_f/SiC -BNNWs composite averages an about 9-% increase compared to that of C_f/SiC composite while the average fracture toughness of the two types of composites are almost equal (as shown in Table 1). It should be acknowledged that such an improvement in the mechanical properties is not as considerable as expected.

To better understand the effect of BNNWs on the mechanical properties of C_f/SiC composites, the fracture surfaces of C_f/SiC -BNNW composites and C_f/SiC composites were studied by means of FESEM. Fig. 3a shows that the fracture surface of the matrix is very smooth in the C_f/SiC composites whereas many slots are clearly observed on the fracture surface of the matrix in the C_f/SiC -BNNW composites, as indicated in Fig. 3b. High-magnification SEM images of these slots are shown in Figs. 3c and d. It is shown that these slots arise from debonding between micro-rods and the matrix and the pullouts of micro-rods, as indicated by white arrows in the images. No apparent debonding and pullouts of BNNWs from the matrix, which are considered to be very beneficial with regard to enhancing the mechanical properties, are found as expected. Nevertheless, there is no denying that the debonding, fracture and pullouts attributable to BNNW-based micro-rods in which a BNNW is deposited by one layer of SiC matrix with the diameter of about 1 μm can also dissipate some fracture energy during crack propagation and contribute to improving the mechanical properties. To evaluate the mechanical properties of the matrix at micron scale, the indentation was made with a triangular diamond pyramidal indenter and then investigated with FESEM. Fig. 4a clearly shows that the matrix in the C_f/SiC composites breaks into pieces after the indentation, exhibiting obvious catastrophic failure as brittle ceramic. On the contrary, the matrix incorporating the BNNWs is not broken and exhibits non-catastrophic failure, as shown in Fig. 4b. Undoubtedly, this result implies that with the introduction of BNNWs, the matrix at micron scale in C_f/SiC composites gains a considerable increase in fracture toughness. However, it is acknowledged that a porous matrix also can absorb a great amount of energy without causing catastrophic failure. As shown in Fig. 4b,

some small pores exist in the matrix. So it is a little confusing with regard to the real reason for such an increase in toughness. To figure out the real toughening mechanisms in the matrix, the crack propagation behavior was investigated. From the high-magnification SEM image (Fig. 4c), the crack propagation behavior in the matrix of C_f/SiC-BNNWs composites is revealed. It can be observed that the main crack in the corner of the triangular indentation is accompanied by many micro-cracks, as pointed out by the white arrows, indicating the occurrence of crack branching. Moreover, these micro-cracks are deflected and then blocked by BNNW-based micro-rods during the propagation, as exhibited in Fig. 4c. In addition, it is also observed that the main crack is deflected by BNNW-based micro-rods during the propagation, as indicated by the white arrows in Fig. 4d. Such crack branching and deflection caused by BNNW-based micro-rods are regarded as the toughening mechanisms and responsible for the non-catastrophic failure of the matrix in C_f/SiC-BNNW composites. To summarize, it is believed that above-mentioned debonding, fracture, pullouts and crack branching and deflection which are ascribed to BNNW-based micro-rods definitely have a positive synergetic effect on the flexural strength and fracture toughness of C_f/SiC composites.

different BNNWs begin to contact each other, forming a whole and dense matrix. So debonding tends to occur between the first and second layer of SiC matrix and thus BNNWs-based micro-rods are observed to pull out and deflect the cracks. Nonetheless, such strengthening and toughening effects originating from BNNW-based micro-rods with the diameter of about 1 μm are believed to be inferior to those of BNNWs that possess a nanoscale effect and more excellent mechanical properties. It may also be the reason for the failure to achieve a significant improvement in the mechanical properties of the composites in this research. Recently, the interphase between the matrix and the reinforcement phase has been deemed a possible approach to relieve the residual thermal stress and optimize interface bonding^{12,29}. In the work on SiC_f/SiC composites reinforced with SiC nanowires⁸, a thin (about 5 nm) carbon interphase was deposited on the nanowires to tailor the interface bonding strength. But debonding and pullouts of SiC nanowires were still not observed. The authors explained that such a thin carbon coating was insufficient to produce sound bonding strength⁸. Hence, considering that no interphase is deposited on the BNNWs in our study, the weak improvement in mechanical properties is not surprising. And it is envisaged that there is a plenty of room for further improvement of the mechanical properties. In our future study, relatively thick carbon interphase or other effective interphases will be deposited on the surfaces of BNNWs to tailor the interface bonding between the BNNWs and the matrix, which is expected to bring about a considerable improvement in the mechanical properties of composites.

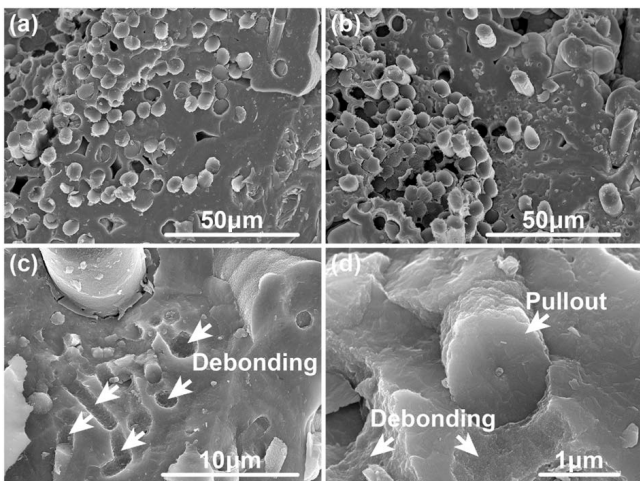


Fig. 3: SEM images of the fracture surfaces of (a) C_f/SiC composites and (b-d) C_f/SiC-BNNWs composites. Debonding and pullouts of micro-rods are clearly observed in the C_f/SiC-BNNWs composites.

However, the reason for the absence of debonding, pullouts, crack deflection etc. from BNNWs in this paper is worthy of further consideration. According to the results reported by other researchers^{8,12,28-30}, it may result from a strong interface bonding between the BNNWs and the matrix. The interface bonding strength comes from the residual thermal stress and/or chemical bonding between the matrix and the reinforcement phase²⁸. Given that BN is chemically stable and it is hard to generate an interface reaction between BN and SiC, the residual thermal stress may be responsible for the very tight bonding owing to the difference in the coefficient of thermal expansion of the SiC matrix and that of the BNNWs. By contrast, the interface bonding between each layer of CVI-SiC matrix is weak. From the second CVI process, the deposited SiC layers on

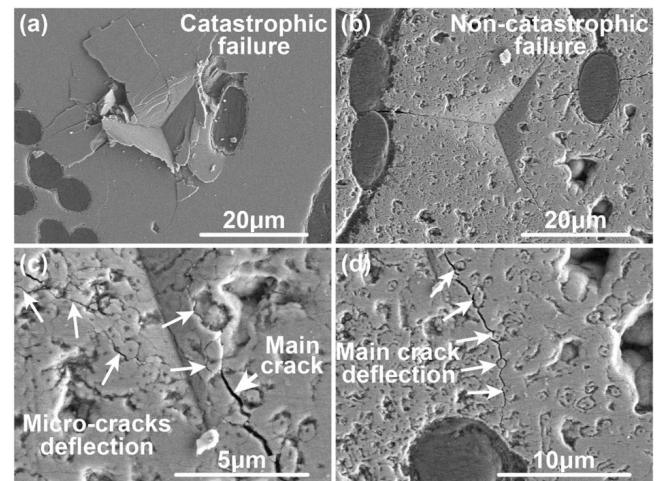


Fig. 4: Low-magnification SEM images of the indentations in the matrix of (a) C_f/SiC composites and (b) C_f/SiC-BNNWs composites. High-magnification SEM images of crack propagation behavior in the matrix of C_f/SiC-BNNWs composites, showing (c) crack branching and (d) crack deflection.

IV. Conclusions

Boron nitride nanowires (BNNWs) were first grown *in situ* into fiber preform with a simplified ball milling, impregnation and annealing method using h-BN powder as raw material. C_f/SiC composites reinforced with these

BNNWs were then fabricated using the CVI method. The as-grown BNNWs exhibit a filled nanostructure with a diameter of 50–180 nm and length of 1–50 μm . Co catalyst particles are observed at the tips of the BNNWs. With the incorporation of BNNWs, the matrix at micron scale in the C_f/SiC composites is toughened notably as evidenced by the results of indentation tests. However, no increases in the flexural strength and fracture toughness of the C_f/SiC composites are observed, owing to the decreased density of the C_f/SiC composites. After normalization by density, the mechanical properties are improved slightly. Debonding, fracture, pullouts and crack branching and deflection, which are attributed to BNNW-based micro-rods are observed. It is believed that such strengthening and toughening mechanisms definitely have a positive synergetic effect on the mechanical properties of C_f/SiC composites. The failure to achieve a significant improvement in the mechanical properties of composites may be caused by the absence of debonding, pullouts, crack deflection, etc. from BNNWs. This is attributable to a strong interface bonding between the BNNWs and the matrix owing to residual thermal stress. Further improvement in the mechanical properties could be obtained by tailoring the interface between the matrix and the BNNWs.

Acknowledgements

This work is supported by the National Natural Science Foundation of China (Grant No. 51502323 and 51172256), Shanghai Key Project of Basic Research (Grant No. 14JC1406200) and Shanghai Scientific Research Project (Grant No. 13521101203).

References

- Schmidt, S., Beyer, S., Knabe, H., Immich, H., Meistring, R., Gessler, A.: Advanced ceramic matrix composite materials for current and future propulsion technology applications, *Acta Astronaut.*, **55**, 409–420, (2004).
- Naslain, R.: Design, preparation and properties of non-oxide CMCs for application in engines and nuclear reactors: An overview, *Compos. Sci. Technol.*, **64**, 155–170, (2004).
- Krenkel, W.: Ceramic matrix composites: Fiber reinforced ceramics and their applications. Wiley-VCH, Weinheim, 2008.
- Naslain, R.R.: The design of the fibre-matrix interfacial zone in ceramic matrix composites, *Composites Part A*, **29**, 1145–1155, (1998).
- Yang, W., Kohyama, A., Katoh, Y., Araki, H., Yu, J., Noda, T.: Effect of C and SiC/C interlayers on mechanical behavior of Tyranno-SA fiber-reinforced SiC matrix composites, *J. Am. Ceram. Soc.*, **86**, 851–856, (2003).
- Naslain, R.R., Paillet, R.J.F., Lamon, J.L.: Single- and multilayered interphases in SiC/SiC composites exposed to severe environmental conditions: An overview, *Int. J. Appl. Ceram. Tec.*, **7**, 263–275, (2010).
- Jia, Y., Li, K., Xue, L., Ren, J., Zhang, S., Zhang, X.: Microstructure and mechanical properties of carbon fiber reinforced multilayered $(\text{PyC-SiC})_n$ matrix composites, *Mater. Des.*, **86**, 55–60, (2015).
- Yang, W., Araki, H., Kohyama, A., Thaveethavorn, S., Suzuki, H., Noda, T.: Process and mechanical properties of *in situ* silicon carbide-nanowire-reinforced chemical vapor infiltrated silicon carbide/silicon carbide composite, *J. Am. Ceram. Soc.*, **87**, 1720–1725, (2004).
- Qian, H., Greenhalgh, E.S., Shaffer, M.S., Bismarck, A.: Carbon nanotube-based hierarchical composites: A review, *J. Mater. Chem.*, **20**, 4751–4762, (2010).
- Chou, T.W., Gao, L., Thostenson, E.T., Zhang, Z., Byun, J.H.: An assessment of the science and technology of carbon nanotube-based fibers and composites, *Compos. Sci. Technol.*, **70**, 1–19, (2010).
- Hu, J., Dong, S., Zhang, X., Zhou, H., Wu, B., Wang, Z., Gao, L.: Process and mechanical properties of carbon/carbon-silicon carbide composite reinforced with carbon nanotubes grown *in situ*, *Composites Part A*, **48**, 73–81, (2013).
- Hu, J., Dong, S., Feng, Q., Zhou, M., Wang, X., Cheng, Y.: Tailoring carbon nanotube/matrix interface to optimize mechanical properties of multiscale composites, *Carbon*, **69**, 621–625, (2014).
- Sun, K., Yu, J., Zhang, C., Zhou, X.: *In situ* growth carbon nanotube reinforced SiC_f/SiC composite, *Mater. Lett.*, **66**, 92–95, (2012).
- Zhi, C.Y., Bando, Y., Wang, W.L.L., Tang, C.C., Kuwahara, H., Golberg, D.: Mechanical and thermal properties of poly-methyl methacrylate-BN nanotube composites, *J. Nanomater.*, **2008**, 1–5, (2008).
- Huo, K.F., Hu, Z., Chen, F., Fu, J.J., Chen, Y., Liu, B.H., Ding, J., Dong, Z.L., White, T.: Synthesis of boron nitride nanowires, *Appl. Phys. Lett.*, **80**, 3611–3613, (2002).
- Chen, Y.J., Chi, B., Mahon, D.C., Chen, Y.: An effective approach to grow boron nitride nanowires directly on stainless-steel substrates, *Nanotechnology*, **17**, 2942–2946, (2006).
- Qiu, Y.J., Yu, J., Rafique, J., Ying, J., Bai, X.D., Wang, E.: Large-scale production of aligned long boron nitride nanofibers by multijet/multicollector electrospinning, *J. Phys. Chem. C*, **2009**, 11228–11234, (2009).
- Ahmad, P., Khandaker, M.U., Khan, Z.R., Amin, Y.M.: A simple technique to synthesize pure and highly crystalline boron nitride nanowires, *Ceram. Int.*, **40**, 14727–14732, (2014).
- Zhi, C.Y., Bando, Y., Tang, C.C., Golberg, D.: Boron nitride nanotubes, *Mater. Sci. Eng., R*, **70**, 92–111, (2010).
- Pakdel, A., Zhi, C.Y., Bando, Y., Golberg, D.: Low-dimensional boron nitride nanomaterials, *Mater. Today*, **15**, 256–265, (2012).
- Zhi, C.Y., Bando, Y., Tang, C.C., Huang, Q., Golberg, D.: Boron nitride nanotubes: Functionalization and composites, *J. Mater. Chem.*, **18**, 3900–3908, (2008).
- Lahiri, D., Hadjikhani, A., Zhang, C., Xing, T., Li, L.H., Chen, Y., Agarwal, A.: Boron nitride nanotubes reinforced aluminum composites prepared by spark plasma sintering: microstructure, mechanical properties and deformation behavior, *Mater. Sci. Eng., A*, **574**, 149–156, (2013).
- Zhu, G., Dong, S., Hu, J., Kan, Y., He, P., Gao, L., Zhang, X., Zhou, H.: *In situ* growth behavior of boron nitride nanotubes on the surface of silicon carbide fibers as hierarchical reinforcements, *RSC Adv.*, **6**, 14112–14119, (2016).
- Chen, Y., Chadderton, L.T., Gerald, J.F., Williams, J.S.: A solid-state process for formation of boron nitride nanotubes, *Appl. Phys. Lett.*, **74**, 2960–2962, (1999).
- Chadderton, L.T., Chen, Y.: Nanotube growth by surface diffusion, *Phys. Lett. A*, **263**, 401–405, (1999).
- Zhang, H., Yu, J., Chen, Y., Fitz Gerald, J.: Conical boron nitride nanorods synthesized via the ball-milling and annealing method, *J. Am. Ceram. Soc.*, **89**, 675–679, (2006).
- Tatarko, P., Grasso, S., Chlup, Z., et al.: Toughening effect of multi-walled boron nitride nanotubes and their influence on the sintering behaviour of 3Y-TZP zirconia ceramics, *J. Eur. Ceram. Soc.*, **34**, 1829–1843, (2014).
- Wang, W.L., Bi, J.Q., Wang, S.R., Sun, K.N., Du, M., Long, N.N., Bai, Y.J.: Microstructure and mechanical properties of alumina ceramics reinforced by boron nitride nanotubes, *J. Eur. Ceram. Soc.*, **31**, 2277–2284, (2011).

- ²⁹ Yang, W., Araki, H., Tang, C., Thaveethavorn, S., Kohyama, A., Suzuki, H., Noda, T.: Single-crystal SiC nanowires with a thin carbon coating for stronger and tougher ceramic composites, *Adv. Mater.*, **17**, 1519–1523, (2005).
- ³⁰ Tatarko, P., Grasso, S., Porwal, H., Chlup, Z., Saggari, R., Dlouhý, I., Reece, M.J.: Boron nitride nanotubes as a reinforcement for brittle matrices, *J. Eur. Ceram. Soc.*, **34**, 3339–3349, (2014).

